# ZMP Fuzzy Implementation for Robot Stability Optimization

*by* Inda Rusdia Sofiani

**Submission date:** 21-Jun-2023 11:04AM (UTC+0700)
**Submission ID:** 2120106049
**File name:** ZMP_Fuzzy_Implementation_for_Robot_Stability.pdf (458.39K)
**Word count:** 3112
**Character count:** 15742

# ZMP Fuzzy Implementation for Robot Stability Optimization

Inda Rusdia Sofiani[a)], Nurkasan[b)], Ghufron Wahyu Kurniawan[c)]

*Department of Electrical Engineering, Universitas Muhammadiyah Malang, Indonesia*

Corresponding author: [a)] indarusdias05@umm.ac.id
[b)]nurkasan@umm.ac.id
[c)]ghufronwahyukurniawan@gmail.com

**Abstract**. One type of robot is a robot with legs that can freely move in all directions and fields representing a human-like form. In a robot movement system, stability and balance present fundamental problems that often arise decreasing the robot's performance especially in robots utilizing feet as a moving medium. The number of legs dramatically affects the balance of the robot. Smaller number of legs generates smaller stability and balance, leading to more significant flexibility. Therefore, this research aims to highlight the stability and balancing, recently alleged as an important topic. The results of this study are in the form of algorithms or methods which create the robot movement in a balanced manner preventing from effortless fall, performed through Zero Moment Point or ZMP. In this study, the authors analyzed the balance of a humanoid robot by paying attention to the robot's Zero Moment Point using Fuzzy. When the robot is walking in place, the robot is not moving or when the robot is walking. This humanoid robot has two legs -called bipedal, demonstrating a lower balance level than other legged robots. It is thus possible to analyze and conduct further development in the present and future, by using the ZMP, anticipated that robot can move without slipping of more than 1 meter

## INTRODUCTION

ZMP (Zero Moment Point) has gained an immense interest for exploration in robot research. This research was initiated with the difficulty in controlling the leg movements of a moving object. The moving object is greatly influenced by the number of energies for each leg. The power from each of the robot's legs is similar to one force. If the party falls within the ZMP area, that point has a moment of inertia equal to zero [1]. In other words, the inertia force must fall within the ZMP area. Thus, the stability of the robot is maintained [2][3].

Several countries such as Japan, Germany, and the United States have researched by specializing in humanoid robots whose progress has been extraordinary. HRP (Humanoid Robot Project), developed by AIST in Japan, has reached a maximum walking speed of 2.5 km/hour supported by the robot's ability to stand stable for a specific period of time [4]. In Germany, the Technische Universität München (TUM) has developed humanoid robots named Johnnie and Lola [5]. MIT Laboratory Leg developed a four-legged robot named Big Dog in collaboration with Boston Dynamics [6].

In this study, the authors analyzed the balance of a humanoid robot by focusing attention to the robot's Zero Moment Point. When the robot is walking in a place, the robot is not moving or when the robot is walking. This research chose humanoid robot because the minimum number of legs on the robot is two or so-called bipedal. This bipedal robot has a lower balance level than robots in general. Therefore, it is possible to analyze and conduct further development in the present and future.

This robot is designed as a half body (limited from leg to hip) with a total number of joints that can move or rotate of as much as 10 degrees of flexible movement. Each leg has 5 degrees of flexibility, with a full robot height of 28.2 cm and a width of 10.2 cm. When the robot is in standing position, the size of the robot becomes 27.7cm. Digital Servo type RDS-3135 builds each joint. In addition, Required Torque is applied to adjust the type of servo with 10 degrees of flexibility. Thus, the robot leg can move flexibly and stably, the 5 DOF on each leg represents two joints in the hip (for top-down and right-left rotation), one joint in the knee, and two joints in the ankle.

## System Planning

This chapter discusses the system design for humanoid robot stability using artificial neuro-fuzzy. The system design is illustrated by using the block diagram in Figure 1.

There are two types of kinematics in controlling the robot motion, which are forward kinematic and inverse kinematic. Forward kinematic calculation navigates the end effector coordinate based on the predetermined angle for each part of the robot's leg. Meanwhile, the inverse kinematic analysis navigates the joint's angle in each part of the robot's leg based on the end-effector. In this final project, control in the motion of the end effector is based on gait and trajectory. Therefore, the utilized kinematics is inverse kinematic.

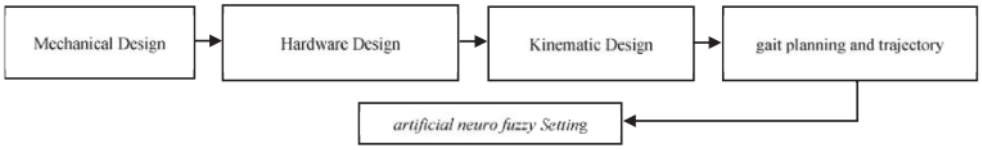


**FIGURE 1.** Block Diagram

In Figure 2, θ1 is the hip joint. θ2 is the joint on the knee. Meanwhile, θ3 is the joint at the ankle. In this robot, all joint movements in the side projection rotate on the Y axis. The following formula in Equation 1 and Equation 2 illustrates the cosine law.

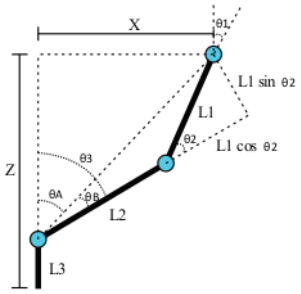


**FIGURE 2.** The right leg of the robot is projected from the side

$$\cos\theta 2 = \frac{R^2 - L1^2 - L2^2}{2 * L1 * L2} \tag{1}$$

$$\theta 2 = arc\cos\left(\frac{R^2 - L1^2 - L2^2}{2 * L1 * L2}\right) \tag{2}$$

Using Pythagoras compute the R that described in Equation 3:

$$R = \sqrt{X^2 * (Z - L3)^2} \tag{3}$$

The next step is conducted to calculate the angle θ3 using Equation 4:

$$\theta 3 = \theta A + \theta B \tag{4}$$

Meanwhile, θA and θB are calculated based on basic trigonometric theory, thereby obtaining Equation 5 and Equation 6.

$$\cos\theta A = \frac{Z}{R} \tag{5}$$

$$\tan\theta B = \frac{L1\sin\theta 2}{L2 + L1\cos\theta 2} \tag{6}$$

Thus resulting Equation 7 and Equation 8:

$$\theta A = arc\cos\frac{Z}{R} \tag{7}$$

$$\theta B = arc\tan\frac{L1\sin\theta 2}{L2 + L1\cos\theta 2} \tag{8}$$

After obtaining the angles from θ3 and θ2, using Equation 9 find θ1

$$\theta 1 = -\theta 2 - \theta 3 \tag{9}$$

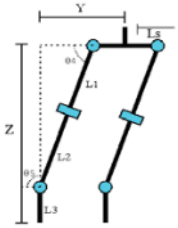


**FIGURE 3.** Projection of the robot's legs from the front

Figure 3 indicates the legs of a humanoid robot with front view projections. θ4 represents the hip joint. Meanwhile, θ5 represents the joint of the ankle. In this robot, all joints in the front projection rotate about the X-axis. θ4 and θ5 determination is employed by using the basic trigonometric theory from Equation 10 and Equation 11.

$$\theta 4 = \frac{\pi}{2} + arc\tan\frac{y - Ls}{Z - L3} \tag{10}$$

$$\theta 5 = \pi - \theta 4 \tag{11}$$

## Gait Design and Trajectory Planning

There are 4 stages of gait pattern to support humanoid robot in walking more stably, illustrated as follows.

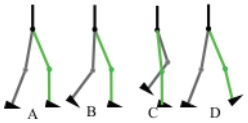


**FIGURE 4**. Steps in humanoid robot leg movement

Figure 4 part A contains a double support phase (DSP) stage. In this condition, both feet are in the wise plane. In the second stage (Figure 4-part B), acknowledged as the pre-swing phase, this condition occurs when the hind legs begin to be lifted. The third stage (Figure 4-part C), is the single support phase, is a condition where one foot is upward so that only one foot touches the footing field. In this part, the body also follows the movement by slowly shifting towards the front. The last is the post-swing phase. At this stage, the leg returns down and slowly begins to touch the area where it is back on. Equations 12, Equation 13, and Equation 14. Depict movement pattern.

$$X_{trajectory(t)} = \frac{Lmove}{Ts}\left(\frac{2\pi t}{Ts} - \sin\left(\frac{2\pi t}{Ts}\right)\right) \tag{12}$$

$$Z_{trajectory(t)} = \frac{h}{2}\left(1 - \sin\left(\frac{2\pi t}{Ts}\right)\right) \tag{13}$$

$$Body_{trajectory(t)} = \frac{Lmove/2}{Ts}\left(\frac{2\pi t}{Ts} - \sin\left(\frac{2\pi t}{Ts}\right)\right) \tag{14}$$

where Xtrajectory(t) is the path of the foot's forward motion (in this case, the X-axis), Ztrajectory(t) is the trajectory of the foot tip upward (in this robot is the Z-axis), Body trajectory is the trajectory of motion of the hips towards the front, L move is The length of the track skipped in a step period, h is the height of the footsteps, Ts is the time required in one step of a period, and t is the time required in each step until Ts is meet. To further clarify, Equation 11, Equation 12, and Equation 13 are depicted as in Figure 5 (a). Robot balancing is required on the right and left sides to avoid the robot falling in a sideward direction, as illustrated Figure 5 (b).

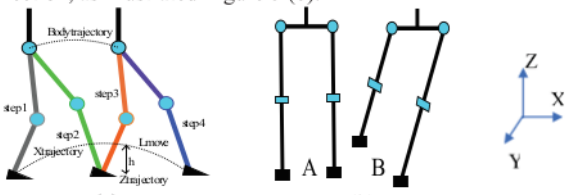


(a) (b)

**FIGURE 5.** Side view of the humanoid robot footpath

Figure 5 (b) illustrates when both legs are in a double support phase (both feet are on), to erect the robot body. Meanwhile, when the right leg is lifted, it prevents the robot from falling and the leg position remains on the polygon support, helping the robot's body to lean on the left side. Thus, the path the robot body on the Y axis is formulated as follows Equation 15.

$$Y_{trajectory(t)} = \frac{Ls}{Ts}\left(\frac{2\pi t}{Ts} - \sin\left(\frac{2\pi t}{Ts}\right)\right) \quad (15)$$

where Ls is the robot's width is divided by 2, Ts is the period of time ledge in one cycle, and T denotes time until it reaches Ts.

## Rule Base And Fuzzy Inference

Fuzzification contains the process of converting numerical data from sensor input into fuzzy sets [9]. Fuzzification, in this final project, utilizes the five sets of supports. With each supporting set, there are 5 errors and a derivative error. The supporting set in this final project utilizes the triangle activation function, illustrated in Figure 6.

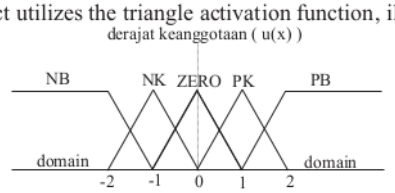


**FIGURE 6.** Fuzzy membership set

NB = Big Negative. NK = Smaller Negative. PK = Smaller Positive. PB = Bigger Positive

In this system, Fuzzy Inference utilizes the Mamdami method where the output of the fuzzy rules utilizes the MIN (minimum) function. Meanwhile, the output from fuzzy is referenced by employing the MAX function (maximum). After obtaining the fuzzy set, the next step is to navigate the rule base by referring to the Macvicar Wheelan Table 1.

**TABLE 1.** Rule Base based on Macvicar Wheelan

| | | Error | | | |
|---|---|---|---|---|---|
| | 0 | 0 | 0 | 1 | 2 |
| Derivative Error | 0 | 0 | 1 | 2 | 3 |
| | 0 | 1 | 2 | 3 | 4 |
| | 1 | 2 | 3 | 4 | 4 |
| | 2 | 3 | 4 | 4 | 4 |

All previous layer values are normalized and converted into 0 and 1 by dividing the input value to simplify the calculation, formulated in Equation 16:

$$output_{ternomasi}[i] = \frac{input[i]}{input[1] + input[2] + \cdots . + input[n]} \quad (16)$$

where $output_{ternomasi}[i]$ is the ith output (iteration) results of normalization, $input[i]$ is input to i (iteration) which will be normalized, and $input[n]$ is input from the last data to be normalized.

The value of the Consequent Parameters includes the set used to recalculate or revise the 4th layer. This revision serves as the center of the bigger or smaller area. Thus, neuro-fuzzy conduct the learning process. The consequent parameter is described in Equation 17:

$$w_i f_i = w_i(p_i x + q_i y + r_i) \quad (17)$$

Where $w_i$ is the value that has been normalized in the iteration I, $f_i$ is the consequent parameter in 4 iteration, and $p_i$ , $q_i$, $r_i$ is the consequent parameter in the first-order model

## Defuzzification

This process aims to return the fuzzy logic values to real values. The utilized technique serves as the center of gravity method. The set of centers of gravity presents a learning tool for artificial neural networks. In this final project, seven sets of outputs are utilized as illustrated in Figure 7.

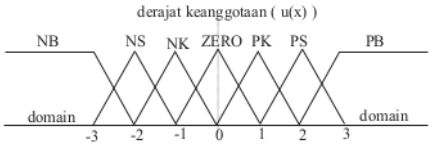


**FIGURE 7.** Defuzzification

With $w_i$ is the value that has been normalized in the iteration i and $f_i$ is consequent for the parameter on the iteration to I, the defuzzification equation is illustrated by Equation 18:

$$\sum i\, w_i\, f_i = \frac{\sum i\, w_i\, f_i}{\sum i\, w_i} \tag{18}$$

## Backpropagation

In this system, the calculation of the error value is directly conducted by comparing the error value of neuro-fuzzy output with the expected value, illustrated by Equation 19presenting the revised weights, as follows.

$$f_i = f_{i-1} + l_r * e * w_i \tag{19}$$

where $f_i$ is consequent parameter (present), $f_{i-1}$ is consequent parameter (past), $l_r$ is learning rate, and $e$ is error (obtained from reference (SP) - defuzzification output)w_i=normalized output.

# RESULT AND DISCUSSION

## Humanoid Servo Controller testing

A digital oscilloscope indicates how the hardware work. The use of this digital oscilloscope allows the researchers to accurately navigate the wave results and measurement results. In this test, the four experiments are conducted with a trigger time (t_on), variously ranging between 1500 uS to 2400 uS, and a period of 10000 uS (10 mS). This limitation is selected as it adjusts to the specifications of the servo motor. The results of the humanoid servo controller hardware testing are presented in Table 2.

**TABLE 2.** The testing results of measurement and humanoid servo controller

| Input controller | | Ouput controller | | Error | Error |
|---|---|---|---|---|---|
| Period (uS) | t_on (uS) | Period(uS) | t_on (uS) | Period (uS) | t_on (uS) |
| 10.000 | 1.500 | 10.120 | 1.530 | 1,20 % | 2,00 % |
| 10.000 | 1.800 | 10.120 | 1.810 | 1,20 % | 0,55 % |
| 10.000 | 2.100 | 10.120 | 2.110 | 1,20 % | 0,47 % |
| 10.000 | 2.400 | 10.120 | 2.410 | 1,20 % | 0,41 % |
| Average error | | | | 1,22 % | 0,68 % |

Table 2 and Figure 8 indicate that the controller demonstrates good results with error of 1,22% in the period and 0.68% for t_on

(a) (b)

**FIGURE 8.** (a) Photo of measurement results at a period of 10 ms and T on 1.5 m, (b) Photo of measurement results at a period of 10 ms and T_on 1.8 ms

## Gait Trajectory Testing

STM Studio monitors the test trajectory. The robot's trajectory, the Z-axis trajectory, the X-axis trajectory, and the Y-axis trajectory serve as the three axes in the robot's trajectory. In this robot, the Z direction indicates the movement

of the legs up and down. The X-axis indicates the robot's motion towards the front or back. Meanwhile, the Y-axis indicates the direction of the robot to the right and left.

## Z Trajectory Testing

Z-axis trajectory (Z-axis) testing occurs by deactivating the X and Y trajectories causing the robot to walk in place. Thus, data can be retrieved and not interfered with by trajectory patterns on other axes.

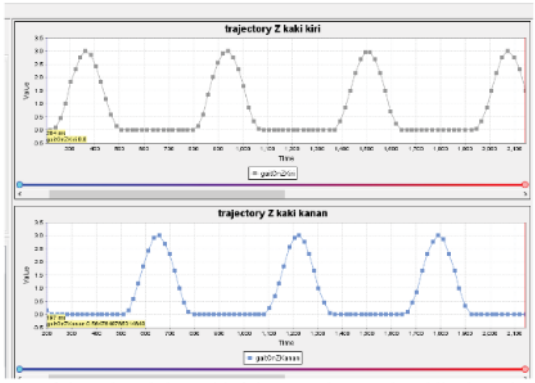


**FIGURE 9.** Trajectory of the robot right and left legs on the Z-axis while the robot is walking in place

Figure 9 indicates the motion of the right and left legs up and down, demonstrating alternately movement. The goal of such movement is to keep one leg on the floor when the other leg moves upwards. The waveform result in Figure 20 demonstrates conformity to the Z trajectory as designed in Chapter 3, which is semi-sinusoidal in shape.

## Y Trajectory Testing

The right and left movement of the robot trajectory implementation is illustrated in Figure 10. Y-axis trajectory test deactivates the X and Z trajectories, and the robot's body swing to right and left is alike an inverted pendulum (inverse pendulum). This condition thus maintains balance and center of gravity which remains on the polygon support or the robot's foothold.

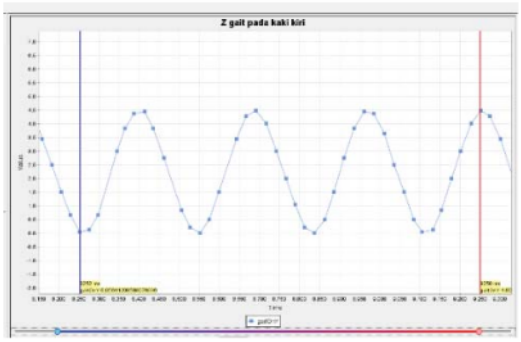


**FIGURE 10.** The trajectory movement of the right and left legs on the Y-axis

The sinusoidal pattern seems rigid as the relatively few steps in one cycle generates the number of steps in one cycle (step in a cycle) which is excessive, burdening the computation process on the microcontroller.

## X Trajectory Testing

The legs move to swing forward and backward alternately between the right and left legs in the X-axis trajectory. The results of the implementation of this trajectory are illustrated in Figure 11. X-axis trajectory test deactivates the Y and Z trajectories. This process eliminates interventions from trajectories on other axes. Meanwhile, Figure 12 also

illustrates the movement of the right and left legs towards the front alternately. The movement in this trajectory also illustrates the suitability between the design and implementation results.

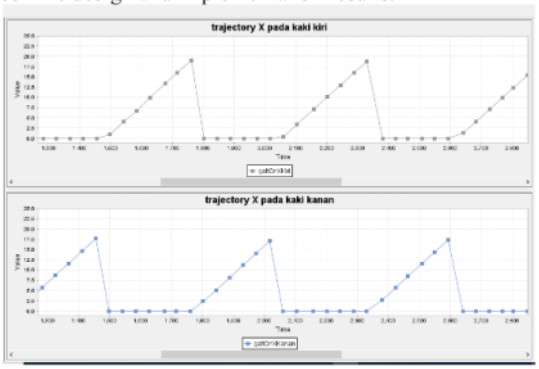


**FIGURE 11.** Trajectory of the robot's right and left legs on the X-axis

## Balancing Testing without balancing control

The experiments investigate the balance test of the robot without neuro-fuzzy, in which the results are presented in Table 3.

**TABLE 3.** Robot balance test results without neuro-fuzzy control

| Experiments | Distance | Robot Status |
|---|---|---|
| 1 | 1 meter | Slip |
| 2 | 1 meter | Slip |
| 3 | 1 meter | Slip |
| 4 | 1 meter | Slip |
| 5 | 1 meter | Slip |

The graph of the monitor presents results of the robot movement, as illustrated in Figure 12.

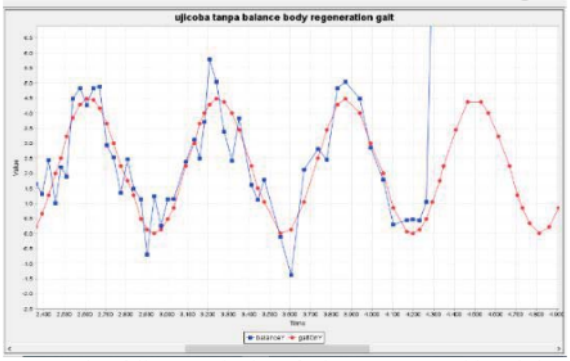


**FIGURE 12.** Results of direct monitoring of robot movement without balance control

The red color on the chart indicates a walking pattern or gait pattern, similarly adjust to the trajectory on the Y-axis. Meanwhile, the blue color indicates the movement of the robot while walking. An Accelerometer-type MPU6050 is attached to the robot's hip to monitor the activity of the robot.

Figure 13 indicates that robots' movement tends to have a high level of interference when following the motion pattern of a given trajectory. In the next several cycles, the blue line rapidly moves away from the red line, indicating the robot falling. Therefore, stabilization is required to keep the robot from falling while walking.

Neuro-fuzzy feedback is based on the pitch and roll gyroscope module of the MPU6050 installed on the robot. In the balance test of the robot without neuro-fuzzy control, the five experiments are presented. The results of these experiments are illustrated in Table 4.

The red color in the graph illustrated in Figure 14 presents the gait or trajectory pattern on the Y-axis. Meanwhile, the blue line indicates the movement of the robot. The graph indicates that the blue line tends to follow the movement of the red line, clarifying a more stable condition.

**TABLE 4.** The results of the robot balance test using neuro-fuzzy control

| Experiments | Distance | Robot Status |
|---|---|---|
| 1 | 1 meter | Safe |
| 2 | 1 meter | Slip |
| 3 | 1 meter | Safe |
| 4 | 1 meter | Safe |
| 5 | 1 meter | Safe |

Meanwhile, the graph of the monitor results when the robot moves is illustrated in Figure 13.

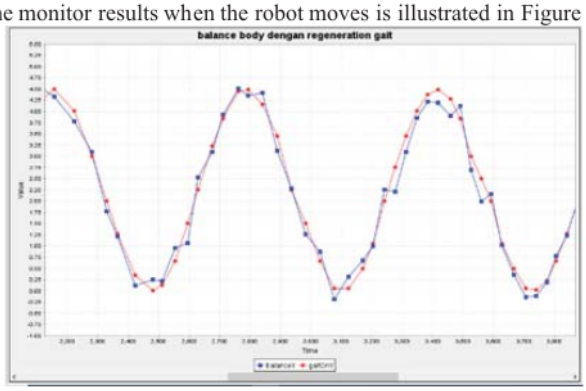


**FIGURE 13.** The results of monitoring the robot movement, directly with balance control using ANFIS.

## CONCLUSION

The humanoid robot stability towards zero moment point based on an artificial neuro-fuzzy inference system has been successfully implemented. From conducted the experiments, the hardware part presents good results, with a small average error value. Further, the trajectory test clarifies the conformity of the products with the design. Meanwhile, in testing the robot balance while walking, the use of neuro-fuzzy controls makes the robot to be more stable and less prone to falling.

## REFERENCES


1. M. VUKOBRATOVIĆ and B. BOROVAC, "Zero-Moment Point — Thirty Five Years Of Its Life," *International Journal of Humanoid Robotics*, **01**, 157–173 (2004),
2. H. Hemami and Y.-F. Zheng, "Dynamics and Control of Motion on the Ground and in the Air with Application to Biped Robots," *Journal of Robotic Systems*, **1**, 101–116 (1984),
3. R. E. Goddard and Y. F. Zheng, "Control of the heel off to toe off motion of a dynamic biped gait," in *Fifth International Conference on Advanced Robotics 'Robots in Unstructured Environments*, 735–744 vol.1 (1991).
4. K. Kaneko *et al.*, "Humanoid robot hrp-4-humanoid robotics platform with lightweight and slim body," in *2011 IEEE/RSJ International Conference on Intelligent Robots and Systems*, 4400–4407 (2011).
5. S. Lohmeier, T. Buschmann, H. Ulbrich, and F. Pfeiffer, "Modular joint design for performance enhanced humanoid robot LOLA," in *Proceedings 2006 IEEE International Conference on Robotics and Automation, 2006. ICRA 2006.*, 88–93 (2006).
6. M. Raibert, K. Blankespoor, G. Nelson, and R. Playter, "Bigdog, the rough-terrain quadruped robot," *IFAC Proceedings Volumes*, **41**, 10822–10825 (2008).

# ZMP Fuzzy Implementation for Robot Stability Optimization

ORIGINALITY REPORT

| 3% | 1% | 2% | 0% |
|---|---|---|---|
| SIMILARITY INDEX | INTERNET SOURCES | PUBLICATIONS | STUDENT PAPERS |

PRIMARY SOURCES

| | | |
|---|---|---|
| 1 | miguelgfierro.com<br>Internet Source | 1% |
| 2 | Ilham Pakaya, Zulfatman, Mochamad Baitur Rizqi. "Improvement reliability index at distribution system in Nguling feeders with recloser placement optimization utilizing genetic algorithm", AIP Publishing, 2022<br>Publication | <1% |
| 3 | Yicheng Zhang, Ling Qin, Jiyao Wang, Wei Xu. "A liquid–solid mixed robot based on ferrofluid with high flexibility and high controllability", Applied Physics Letters, 2022<br>Publication | <1% |
| 4 | Geqi Lin, Wenchuan Jia, Shugen Ma, Jianjun Yuan, Yi Sun. "Research and Analysis of Comprehensive Optimization Method for Energy Consumption and Trajectory Error of the Leg Structure Based on Virtual Model Control", 2021 IEEE International Conference on Mechatronics and Automation (ICMA), 2021<br>Publication | <1% |

| | | |
|---|---|---|
| 5 | M. Vukobratović, B. Borovac, V. Potkonjak. "Towards a unified understanding of basic notions and terms in humanoid robotics", Robotica, 2006<br>Publication | <1 % |
| 6 | Peiqi Wang, Jingde Li, Shubei Wang, Fusheng Zhang, Juanjuan Shi, Changqing Shen. "A new meta-transfer learning method with freezing operation for few-shot bearing fault diagnosis", Measurement Science and Technology, 2023<br>Publication | <1 % |
| 7 | core-cms.prod.aop.cambridge.org<br>Internet Source | <1 % |
| 8 | www.ohio.edu<br>Internet Source | <1 % |
| 9 | Donghyun Kim, Junhyeok Ahn, Orion Campbell, Nicholas Paine, Luis Sentis. "Investigations of a Robotic Test Bed With Viscoelastic Liquid Cooled Actuators", IEEE/ASME Transactions on Mechatronics, 2018<br>Publication | <1 % |
| 10 | infoscience.epfl.ch<br>Internet Source | <1 % |

| | | | |
|---|---|---|---|
| Exclude quotes | On | Exclude matches | Off |
| Exclude bibliography | On | | |

# Digital Receipt

This receipt acknowledges that Turnitin received your paper. Below you will find the receipt information regarding your submission.

The first page of your submissions is displayed below.

| | |
|---|---|
| Submission author: | Inda Rusdia Sofiani |
| Assignment title: | Publication Articles April-Juni 2023 |
| Submission title: | ZMP Fuzzy Implementation for Robot Stability Optimization |
| File name: | ZMP_Fuzzy_Implementation_for_Robot_Stability.pdf |
| File size: | 458.39K |
| Page count: | 8 |
| Word count: | 3,112 |
| Character count: | 15,742 |
| Submission date: | 21-Jun-2023 11:04AM (UTC+0700) |
| Submission ID: | 2120106049 |

**ZMP Fuzzy Implementation for Robot Stability Optimization**

Inda Rusdia Sofiani[a], Nurkasan[b], Ghufron Wahyu Kurniawan[c]

*Department of Electrical Engineering, Universitas Muhammadiyah Malang, Indonesia*

Corresponding author: [a] indarusdia05@umm.ac.id
[b]nurkasan@umm.ac.id
[c]ghufronwahyukurniawan@gmail.com

**Abstract**. One type of robot is a robot with legs that can freely move in all directions and fields representing a human-like form. In a robot movement system, stability and balance present fundamental problems that often arise decreasing the robot's performance especially in robots utilizing feet as a moving medium. The number of legs dramatically affects the balance of the robot. Smaller number of legs generates smaller stability and balance, leading to more significant flexibility. Therefore, this research aims to highlight the stability and balancing, recently alleged as an important topic. The results of this study are in the form of algorithms or methods which create the robot movement in a balanced manner preventing from effortless fall, performed through Zero Moment Point or ZMP. In this study, the authors analyzed the balance of a humanoid robot by paying attention to the robot's Zero Moment Point using Fuzzy. When the robot is walking in place, the robot is not moving or when the robot is walking. This humanoid robot has two legs -called bipedal, demonstrating a lower balance level than other legged robots. It is thus possible to analyze and conduct further development in the present and future, by using the ZMP, anticipated that robot can move without slipping of more than 1 meter

**INTRODUCTION**

ZMP (Zero Moment Point) has gained an immense interest for exploration in robot research. This research was initiated with the difficulty in controlling the leg movements of a moving object. The moving object is greatly influenced by the number of energies for each leg. The power from each of the robot's legs is similar to one force. If the party falls within the ZMP area, that point has a moment of inertia equal to zero [1]. In other words, the inertia force must fall within the ZMP area. Thus, the stability of the robot is maintained [2][3].

Several countries such as Japan, Germany, and the United States have researched by specializing in humanoid robots whose progress has been extraordinary. HRP (Humanoid Robot Project), developed by AIST in Japan, has reached a maximum walking speed of 2.5 km/hour supported by the robot's ability to stand stable for a specific period of time [4]. In Germany, the Technische Universität München (TUM) has developed humanoid robots named Johnnie and Lola [5]. MIT Laboratory Leg developed a four-legged robot named Big Dog in collaboration with Boston Dynamics [6].

In this study, the authors analyzed the balance of a humanoid robot by focusing attention to the robot's Zero Moment Point. When the robot is walking in a place, the robot is not moving or when the robot is walking. This research chose humanoid robot because the minimum number of legs on the robot is two or so-called bipedal. This bipedal robot has a lower balance level than robots in general. Therefore, it is possible to analyze and conduct further development in the present and future.

This robot is designed as a half body (limited from leg to hip) with a total number of joints that can move or rotate of as much as 10 degrees of flexible movement. Each leg has 5 degrees of flexibility, with a full robot height of 28.2 cm and a width of 10.2 cm. When the robot is in standing position, the size of the robot becomes 27.7cm. Digital Servo type RDS-3135 builds each joint. In addition, Required Torque is applied to adjust the type of servo with 10 degrees of flexibility. Thus, the robot leg can move flexibly and stably, the 5 DOF on each leg represents two joints in the hip (for top-down and right-left rotation), one joint in the knee, and two joints in the ankle.

**System Planning**

This chapter discusses the system design for humanoid robot stability using artificial neuro-fuzzy. The system design is illustrated by using the block diagram in Figure 1.